Design and Implementation of an Inverse Dynamics Controller for Uncertain Nonholonomic Robotic Systems

Article *in* Journal of Intelligent & Robotic Systems · July 2013

DOI: 10.1007/s10846-012-9762-x

Khoshnam Shojaei
Najafabad Branch, Islamic Azad University

Alireza Mohammad Shahri
Iran University of Science and Technology

J Intell Robot Syst (2013) 71:65–83
DOI 10.1007/s10846-012-9762-x

Design and Implementation of an Inverse Dynamics Controller for Uncertain Nonholonomic Robotic Systems

Khoshnam Shojaei · Alireza Mohammad Shahri · Behzad Tabibian

Received: 13 April 2011 / Accepted: 26 July 2012 / Published online: 12 August 2012

Abstract This paper addresses the trajectory tracking control problem of nonholonomic robotic systems in the presence of modeling uncertainties. A tracking controller is proposed such that it combines the inverse dynamics control technique and an adaptive robust PID control strategy to preserve robustness to both parametric and nonparametric uncertainties. A SPR-Lypunov stability analysis demonstrates that tracking errors are uniformly ultimately bounded (UUB) and exponentially converge to a small ball containing the origin. The proposed inverse dynamics tracking controller is successfully applied to a nonholonomic wheeled mobile robot (WMR) and experimental results are presented to validate the effectiveness of the proposed controller.

K. Shojaei (✉) · A. M. Shahri
Mechatronics and Robotics Research Laboratory, Electronic Research Center, Electrical Engineering Department, Iran University of Science and Technology, Tehran, Iran
e-mail: khoshnam.shojaee@gmail.com, shojaei@ee.iust.ac.ir

A. M. Shahri
e-mail: shahri@iust.ac.ir

B. Tabibian
School of Informatics, University of Edinburgh, Edinburgh, England
e-mail: s.b.tabibian@sms.ed.ac.uk

Keywords Adaptive-robust · Inverse dynamics control · Nonholonomic systems · Uncertainty · Trajectory tracking

1 Introduction

The motion control problem of mechanical systems subject to nonholonomic constraints has attracted a significant attention during past years [9]. Wheeled vehicles, wheeled mobile robots (WMRs), multi-fingered robotic hands and space robots are typical examples of such systems. According to the basic theorem of Brockett [1], such systems can not be stabilized at any equilibrium configuration by smooth static state feedback. From a review of the literature [9], this well-known theorem and challenging nonlinear nature of nonholonomic systems motivate many researchers to be focused on the motion control problem of such systems. In spite of much effort on the design of stabilizing controllers for nonholonomic systems, limited types of feedback controllers have been developed. Some fundamental results on modeling, control and stabilization of nonholonomic systems have been reported in [3–5]. Some researchers proposed stabilizing controllers for nonholonomic systems by converting them into the chained form [10, 17, 19, 21]. Among various motion control problems of nonholonomic systems, most of researches have been concentrated on the tracking of a geometric path with an associated timing law so-called the trajectory tracking. A variety of control algorithms for the trajectory tracking problem is developed in the literature [8, 18, 19, 21, 29]. Differential geometric control theory may be traditionally utilized to design feedback linearizing controllers to solve trajectory tracking problem of nonholonomic systems [14]. From a review of the literature, following results are summarized with regard to application of this technique for nonholonomic systems: 1. A nonholonomic system is controllable and its equilibrium point can be made Lyapunov stable, but can not be made asymptotically stable by a smooth static state feedback [4]. 2. It has been shown that nonholonomic systems are not input-state linearizable. However, if one chooses a proper set of output equations, it may be input-output linearizable [6, 8]. 3. The dimension of the largest feedback linearizable subsystem of the kinematic and dynamic model of a nonholonomic system is two times of the number of its actuators and the controllability index of each subsystem is equal to 2 [3]. 4. The internal dynamics of these systems are stable [13]. There exists invaluable works that propose trajectory tracking controllers based on feedback linearization for nonholonomic systems which most of them are developed for nonholonomic wheeled mobile robots [3, 8, 15, 20, 22]. However, they use exact kinematic and dynamic model of the nonholonomic systems. Feedback linearization is based on cancellation of nonlinear terms. Therefore, this cancellation may not be achieved perfectly in the presence of uncertainties in nonholonomic robotic systems. In [25], an adaptive feedback linearizing control system was developed to solve this problem for a nonholonomic WMR. The experimental results of the proposed controller in [25] on a real WMR is presented in [27]. However, the computer simulations and real experiments show that the proposed adaptive control system loses its stability in some experiments because of the presence of nonparametric uncertainties such as surface friction and unmodeled castor wheels. Martins et al. [24] proposed an adaptive dynamic tracking controller with sigma-modification for a differential drive WMR. However, the size of the ultimate bound of tracking errors depends on external disturbances and it can not be freely adjusted by control parameters. Furthermore, the transient performance of their proposed controller is not clear. In the previous work [26], these problems are solved by designing of an adaptive robust tracking control law. However, the controller is not experimentally evaluated by a real WMR. Based on the current knowledge of the authors, there is no currently available work to propose inverse dynamics control to solve the trajectory tracking problem of uncertain nonholonomic robotic systems in the presence of both parametric and nonparametric uncertainties. Furthermore, most of proposed robust controllers [16, 21, 26, 28, 30] have not been experimentally evaluated on real nonholonomic robotic systems.

Therefore, the main contributions of the present paper are clearly stated as follows. An adaptive-robust inverse dynamics tracking controller is designed for an integrated kinematic and dynamic formulation of nonholonomic robotic systems in the presence of parametric and nonparametric uncertainties. The work of Sarkar [8] is essential in the development of the controller. In contrast to many available results which employ the backstepping technique in the design of the controller for WMRs, this paper proposes a unified tracking controller which comprises adaptive robust inverse dynamics and robustified PID control laws. The SPR-Lyapunov stability analysis is utilized to demonstrate that the tracking errors are uniformly ultimately bounded (UUB) and exponentially converge to a small ball containing the origin whose radius can be freely adjusted by control parameters. Experimental results on a commercial nonholonomic WMR are presented to evaluate the faesibility of the proposed controller. Since the actuator dynamic is ignored based on the assumption of wheel torques as the input of the robot system in most of the previous researches, it is more reasonable and practical to take into account the actuator input voltages as the control inputs. However, the commercial WMRs may be commanded by velocities and they may not accept the actuator voltages as the input [23, 24]. Das et al. [30] proposed a neuron-based adaptive controller for a nonholonomic WMR including actuator dynamics. However, their proposed controller provides voltage signals as the input and may not be applicable for commercially available WMRs. The proposed controller in the work of Martins et al. [24] considers this problem and provides velocities as the input in the dynamic model of the commercial WMR based on the presented model by De La Cruz and Carelli [23]. In this work, the presented model in [23] is also utilized to provide the feasibility of the experimental evaluation of the proposed controller on a commercial WMR.

The rest of the paper is organized as follows. In Section 2, the kinematic and dynamic model of nonholonomic robotic systems are briefly reviewed and the control objective is stated. Section 3 proposes the trajectory tracking controller and the stability analysis of the closed-loop system. The proposed method is applied to a nonholonomic differential drive WMR in Section 4. Simulation results are also presented in this section in order to evaluate the efficiency of the controller. Section 5 presents experimental results on robuLAB 10 WMR to verify the effectiveness of the proposed control law. Finally, Section 6 concludes the paper.

2 Problem Statement

Consider a class of nonholonomic robotic systems subject to m constraints in the following form [8]:

$$M(q)\ddot{q} + C\left(q,\dot{q}\right)\dot{q} + B(q)F\left(\dot{q}\right) + B(q)\tau_d = B(q)\tau - A(q)^T\lambda, \tag{1}$$

$$A(q)\dot{q} = 0 \tag{2}$$

where $q = \left[q_1, q_2, \ldots, q_n\right]^T$ is a vector of generalized coordinates, $\tau \in \Re^{(n-m)\times 1}$ is the vector of actuators inputs, $M(q) \in \Re^{n\times n}$ is a symmetric positive-definite inertia matrix, $C\left(q,\dot{q}\right) \in \Re^{n\times n}$ is the centripetal and Coriolis matrix, $F\left(\dot{q}\right) \in \Re^{(n-m)\times 1}$ denotes friction vector, $\tau_d \in \Re^{(n-m)\times 1}$ denotes bounded unknown disturbances, $B(q) \in \Re^{n\times(n-m)}$ is the input transformation matrix, $A(q) \in \Re^{m\times n}$ is a full-rank matrix and $\lambda \in \Re^{m\times 1}$ is a vector of Lagrange multipliers which denotes constraint forces. From a review of [8, 16], let $S(q) = \left[s_1(q), s_2(q), \ldots, s_{n-m}(q)\right]^T$ be a full-rank matrix that is made up of a set of smooth and linearly independent vector fields, $s_i(q) \in \Re^n$, $i = 1, \ldots, n-m$, in the null space of $A(q)$ i.e. $A(q).S(q) = 0$. Considering Eq. 2, one may find a vector of pseudo-velocities of the system as $v(t) = \left[v_1(t), v_2(t), \ldots, v_{n-m}(t)\right]^T$ such that

$$\dot{q} = S(q)v(t) = s_1(q)v_1 + \ldots + s_{n-m}(q)v_{n-m} \tag{3}$$

Differentiating Eq. 3 yields $\ddot{q} = \dot{S}(q)v + S(q)\dot{v}$ which is substituted in Eq. 1 and the result is multiplied by $S^T(q)$ to give the following dynamic equation:

$$\overline{M}\dot{v}(t) + \overline{C}\left(q,\dot{q}\right)v(t) + \overline{F}\left(\dot{q}\right) + \overline{\tau}_d = \overline{B}\tau \tag{4}$$

where $\overline{M} = S^T MS$, $\overline{C}\left(q,\dot{q}\right) = S^T M\dot{S} + S^T CS$, $\overline{B} = S^T B$, $\overline{F} = \overline{B}F$, $\overline{\tau}_d = \overline{B}\tau_d$. To consider the actuator dynamics, it is assumed that the robot is actuated by $n-m$ similar brushed DC motors with mechanical gears. The electrical equation of each motor armature is written as follows:

$$u_a = L_a di_a/dt + R_a i_a + k_b \dot{\theta}_m \tag{5}$$

where k_b is the back EMF constant, R_a and L_a denote the resistance and inductance of the motor armature, respectively, and u_a is the voltage input. By ignoring the inductance of armature circuit, and considering the relation between torque and armature current (i.e. $\tau_m = k_\tau i_a$) and relations between torque and velocity before and after gears (i.e. $\tau = n\tau_m$ and $\dot{\theta}_m = n\dot{\theta}$), the delivered torque to the system by actuators is given by:

$$\tau = k_1 u_a - k_2\dot{\theta} \tag{6}$$

where $k_1 = \left(nk_\tau/R_a\right)$, $k_2 = nk_b k_1$, $n = n_w/n_m$ is gear ratio and k_τ is torque constant of the motor. The Eq. 6 may be re-written as:

$$\tau = k_1 u_a - k_2 X_T v, \tag{7}$$

where $X_T \in \Re^{(n-m)\times(n-m)}$ is a transformation matrix which transforms wheels velocities to pseudo-velocities vector. After substituting Eq. 7 in Eq. 4, one obtains:

$$\overline{M}\dot{v}(t) + \left(\overline{C}\left(q,\dot{q}\right) + k_2\overline{B}X_T\right)v(t) + \overline{F}\left(\dot{q}\right) + \overline{\tau}_d = k_1\overline{B}u_a \tag{8}$$

Property 1: $\overline{M}(q)$ is a symmetric and positive-definite matrix which is upper and lower bounded, that is, $\overline{m}_1 \leq \left\|\overline{M}(q)\right\| \leq \overline{m}_2$, where $\overline{m}_1$and $\overline{m}_2$ are positive scalar constants.

Property 2: Following upper bounding functions are valid for the presented kinematic and dynamic models of nonholonomic systems:

$$\|S(q)\| \leq s_1, \left\|\overline{C}\left(q,\dot{q}\right)\right\| \leq \overline{c}_1\|v\|, \left\|\overline{F}\left(\dot{q}\right)\right\| \leq \overline{f}_1 + \overline{f}_2\|v\|, \|\overline{\tau}_d\| \leq \overline{\tau}_1, \tag{9}$$

where s_1, $\overline{f}_1$, $\overline{f}_2$, $\overline{c}_1$ and $\overline{\tau}_1$ are positive scalar constants.

The kinematic model 3 and dynamic equation 8 may be integrated into the following state space representation in companion form:

$$\dot{x} = \begin{bmatrix}\dot{q}\\ \dot{v}\end{bmatrix} = \begin{bmatrix}Sv\\ 0\end{bmatrix} + \begin{bmatrix}0\\ k_1\overline{M}^{-1}\overline{B}\end{bmatrix}u_a + \begin{bmatrix}0\\ -\overline{M}^{-1}\left(\left(\overline{C}\left(q,\dot{q}\right) + k_2\overline{B}X_T\right)v(t) + \overline{F}\left(\dot{q}\right) + \overline{\tau}_d\right)\end{bmatrix} \tag{10}$$

where $x \in \Re^{(2n-m)}$ is the state vector. This representation allows applying the differential geometric control theory for the trajectory tracking problem. Based on the discussed problem, this work will be focused on input-output linearization control technique to solve trajectory tracking problem. Therefore, by choosing an appropriate set of output equations, $y(t) = h(q(t))$, the control objective is stated as follows. Given a smooth bounded reference trajectory $y_r(t) = h(q_r(t))$ which is generated by a reference robot, and assuming that q_r satisfies the velocity constraints 2, then the integrated kinematic and dynamic tracking control problem discussed in this paper is to design a feedback control law for the system 10 with output equation, $y(t) = h(q(t))$, such that it satisfies $\lim_{t\to\infty} e(t) = 0$ where $e(t) = y(t) - y_r(t)$ is the position tracking error. Following assumptions are essential in the development of the controller in the next section.

Assumption 1: Measurements of all states, i.e. $x = \left[q^T, v^T\right]^T$, are available in real-time.

Assumption 2: The reference trajectory $y_r(t)$ is chosen such that $y_r(t)$, $\dot{y}_r(t)$ and $\ddot{y}_r(t)$ are all bounded signals.

Assumption 3: Since kinematic parameters of nonholonomic systems are geometric and easy to measure, such parameters are reasonably assumed to be certain in this paper. However, development of the controller is trivial and straightforward for uncertain kinematic parameters in the next section.

3 Development of the Inverse Dynamics Control

3.1 SPR-Lyapunov Design

This section proposes an adaptive-robust tracking controller based on inverse dynamics technique for the integrated kinematic and dynamic formulation of nonholonomic systems given in Eq. 10. The system 10 may be stated as the following affine multi-input nonlinear model:

$$\dot{x} = f(x) + \sum_{i=1}^{n-m} g_i(x,\theta)\,u_{a\,i} + \xi(x) \tag{11}$$

where $x \in \Re^{(2n-m)}$ and $f(x)$, $g_i(x,\theta)$ and $\xi(x)$ are smooth vector fields on $\Re^{(2n-m)}$ with $g(0,\theta) \neq 0$. The parameter vector $\theta \in \Re^p$ includes uncertain parameters in the input matrix in Eq. 10. The output equations are functions of generalized coordinates q. Since the number of degrees of freedom of the nonholonomic system is instantaneously

$n - m$, one has $n - m$ independent position output equations as:

$$y = h(x) = \left[h_1(q), h_2(q), \ldots, h_{n-m}(q)\right]^T \quad (12)$$

The basic approach to obtain a linear input-output relation is to repeatedly differentiate the outputs so that they are explicitly related to inputs. After differentiating, the following expression is obtained:

$$\begin{aligned}\dot{y}_j &= L_f h_j + L_\xi h_j + \sum_{i=1}^{n-m} \left(L_{g_i} h_j\right) u_{ai} \\ &= J_{h_j}(q)\, S(q)\, v, \quad j = 1, 2, ..., n - m \end{aligned} \quad (13)$$

which it is not related to the actuators input. In Eq. 13, $J_{h_j}(q) = \partial h_j(q) / \partial q$. By differentiating again, it yields:

$$\begin{aligned}\ddot{y}_j &= L_f^2 h_j + L_f L_\xi h_j + L_\xi L_f h_j + L_\xi^2 h_j \\ &\quad + \left(\sum_{i=1}^{n-m} L_{g_i}\left(L_f h_j\right) u_{ai} + \sum_{i=1}^{n-m} L_{g_i}\left(L_\xi h_j\right) u_{ai}\right)\end{aligned} \quad (14)$$

where it is obvious that $L_{g_i}\left(L_f h_j\right) \neq 0$. After some simplifications, Eq. 14 may be re-written for the entire system as:

$$\ddot{y} = L_f^2 h(x) + L_\xi L_f h(x) + L_g L_f h(x)\, u_a \quad (15)$$

where $L_g L_f h(x) := D(x)$ is defined as the decoupling matrix:

$$D(x) = \begin{bmatrix} L_{g_1} L_f h_1 & \ldots & L_{g_{n-m}} L_f h_1 \\ \vdots & \ddots & \vdots \\ L_{g_1} L_f h_{n-m} & \ldots & L_{g_{n-m}} L_f h_{n-m} \end{bmatrix} \quad (16)$$

Assume that the condition $\det(D(x)) \neq 0$ is satisfied. Thus, the system 11 and 12 is input-output linearizable. The following nonlinear feedback

$$u_a = D^{-1}(x)\left(\eta - L_f^2 h(x)\right), \quad (17)$$

linearizes and decouples the system into $n - m$ perturbed double integrators as follows:

$$\ddot{y} = \eta + L_\xi L_f h, \quad (18)$$

where η_j, $j = 1, 2, \ldots, n - m$ represents the new external inputs. It is assumed that there are p unknown parameters in the dynamic model of the nonholonomic system and $L_\xi L_f h(x)$ denotes non-parametric uncertainties. According to certainty equivalence principle, $D(x)$ must be replaced by its estimate in decoupling control law 17

$$u_a = \widehat{D}^{-1}(x)\left(\eta - L_f^2 h\right), \quad (19)$$

where

$$\widehat{D}(x) = L_{\widehat{g}} L_f h(x) \quad (20)$$

Since $f(x)$ and $h(x)$ do not contain any uncertain term and the system states are available for feedback by sensor measurements according to Assumptions 1 and 3, the term $L_f^2 h$ is also available. By substituting Eq. 19 in Eq. 15, the following expression is obtained:

$$\ddot{y} = L_f^2 h(x) + D(x)\, \widehat{D}^{-1}(x)\left(\eta - L_f^2 h\right) + L_\xi L_f h(x) \quad (21)$$

After some manipulation, Eq. 21 can be written in the following form:

$$\ddot{y} = \eta + \widetilde{D}(x)\, \widehat{D}^{-1}(x)\left(\eta - L_f^2 h\right) + L_\xi L_f h(x), \quad (22)$$

where

$$\widetilde{D}(x) = D(x) - \widehat{D}(x) \quad (23)$$

Then, it is assumed that one can write Eq. 22 in the following parametric form:

$$\ddot{y} = \eta + W(x, \eta)\, \widetilde{\theta} + L_\xi L_f h(x) \quad (24)$$

where $\widetilde{\theta} = \left[\widetilde{\theta}_1, \widetilde{\theta}_2, \ldots, \widetilde{\theta}_p\right]^T$ is the vector of parameters estimation errors and the matrix $W \in \Re^{(n-m)\times p}$ is the regression matrix which is made up of time known functions. Considering the structural properties of the nonholonomic robotic systems, this parametric form is achievable for the nonholonomic systems. Now, the adaptive law may be derived by SPR-Lyapunov design approach which is motivated from [2, 12]. Assume that the external control input η_j for j-th subsystem of Eq. 24 is chosen such that j-th output, $y_j(t)$, tracks the desired output, $y_{jr}(t)$, in the outer loop:

$$\eta_j = \ddot{y}_{jr} - k_{pj} e_j - k_{vj} \dot{e}_j - k_{a\,j} \int_0^t e_j(\tau) d\tau + v_{Rj},\quad j = 1, 2, \ldots n - m \tag{25}$$

where k_{pj}, k_{vj}, k_{aj} denote gains of the outer loop controller. The robust control 25 is interpreted as follows:

1. the control term v_{Rj} is a robust control law which must be designed to compensate for nonparametric uncertainty $L_\xi L_f h(x)$,
2. a feedforward control action $\ddot{y}_{jr}$ is to compensate the acceleration of the desired trajectory,
3. a PID feedback controller plays the key role to stabilize the error system which is developed as follows.

Applying the robustified PID control law given in Eq. 25 to j-th subsystem of Eq. 24 leads to the following error equation:

$$\ddot{e}_j + k_{vj} \dot{e}_j + k_{pj} e_j + k_{a\,j} \int_0^t e_j(\tau)\, d\tau = W_j \widetilde{\theta} + \left(L_\xi L_f h(x)\right)_j + v_{R\,j} \tag{26}$$

where $W_j = \left[w_{j1}, w_{j2}, \ldots, w_{jn-m}\right]$ is the j-th row of regression matrix. For the purpose of adaptation, one may use the following filtered error signal for j-th output:

$$\varepsilon_j(t) = \dot{e}_j(t) + \beta_{1j} e_j(t) + \beta_{2j} \int_0^t e_j(\tau)\, d\tau,\quad j = 1, 2, \ldots, n - m \tag{27}$$

Since $\dot{e}_j = \dot{y}_j - \dot{y}_{jr}$ is known as a function of measured states by considering Eq. 13, it is obvious that ε_j is available. The parameters β_{1j} and β_{2j} are chosen such that the transfer function of the closed-loop error system 26 and 27, which is defined form the output $\varepsilon_j(t)$ to the input $\left(W_j\widetilde{\theta} + \left(L_\xi L_f h(x)\right)_j + v_{R\,j}\right)$, will be strictly positive real (SPR):

$$H_j(s) = \left(s^2 + \beta_{1j} s + \beta_{2j}\right) \big/ \left(s^3 + k_{vj} s^2 + k_{pj} s + k_{a\,j}\right) \tag{28}$$

The transfer function $H_j(s)$ is strictly positive real (SPR) based on the following theorem:

Theorem 1 *Assume that a rational function $H_j(s)$ of the complex variable $s = \sigma + j\omega$ is real for real sand is not identically zero for all s. Let n^* be the relative degree of $H_j(s)$ with $|n^*| \le 1$. Then, $H_j(s)$ is SPR if and only if (i) $H_j(s)$ is analytic in Re[s] > 0, (ii) $Re\left[H_j(j\omega)\right] > 0,\ \forall\omega \in (-\infty, \infty)$, (iii) when $n^* = 1$, $\lim_{|\omega|\to\infty} \omega^2 Re\left[H_j(j\omega)\right] > 0$, when $n^* = -1$, $\lim_{|\omega|\to\infty} H_j(j\omega)\big/ j\omega > 0$.*

Proof See the reference [12]. □

By following the presented conditions in the Theorem 1, one may easily show that $H_j(s)$ is SPR if $k_{pj} < k_{vj}^2$, $k_{pj} k_{vj} > k_{a\,j}$, $k_{pj}^2 > 2k_{a\,j} k_{vj}$, $\beta_{1j} = k_{pj}\big/k_{vj}$ and $\beta_{2j} = k_{a\,j}\big/k_{vj}$. The following lemma is essential for the SPR-Lyapunov design in the sequel.

Lemma 1 ((Meyer-Kalman-Yakubovitch)) *Consider the following linear system*

$$\dot{x} = Ax + Bu,$$
$$y = Cx,$$

Then, the system is SPR if and only if: (a) for any symmetric positive-definite Q, there exists a symmetric positive-definite P solution of the Lyapunov equation $A^T P + PA = -Q$. (b) The matrices B and C satisfy $B^T P = C$ [7].

Accordingly, by Lemma 1, there exists positive definite matrices P_j and Q_j such that

$$A_j^T P_j + P_j A_j = -Q_j,\ \ P_j B_j = C_j^T \tag{29}$$

where matrices A_j, B_j and C_j are defined by minimal state space realization of Eqs. 26 and 27 in the following form:

$$\dot{X}_j = A_j X_j + B_j \left(W_j \widetilde{\theta} + \left(L_\xi L_f h(x)\right)_j + v_{R\,j}\right),\quad \varepsilon_j = C_j X_j \tag{30}$$

where $X_j = \left[\int_0^t e_j(\tau)\, d\tau \;\; e_j \;\; \dot{e}_j \right]^T$ is the state variable and

$$A_j = \begin{bmatrix} 0 & 1 & 0 \\ 0 & 0 & 1 \\ -k_{aj} & -k_{pj} & -k_{vj} \end{bmatrix}, \; B_j = \begin{bmatrix} 0 \\ 0 \\ 1 \end{bmatrix},$$
$$C_j = \left[\beta_{2j} \; \beta_{1j} \; 1 \right]. \tag{31}$$

As a result, the error equation for the entire system is written as:

$$\dot{X} = AX + B\left(W\widetilde{\theta} + L_\xi L_f h(x) + v_R\right), \; E_1 = CX \tag{32}$$

where $A \in \Re^{3(n-m)\times 3(n-m)}$, $B \in \Re^{3(n-m)\times(n-m)}$ and $C \in \Re^{(n-m)\times 3(n-m)}$ are block diagonal matrices:

$$A = diag\left(A_1, A_2, \ldots, A_{n-m}\right),$$
$$B = diag\left(B_1, B_2, \ldots, B_{n-m}\right),$$
$$C = diag\left(C_1, C_2, \ldots, C_{n-m}\right), \tag{33}$$

and $X = \left[X_1^T, \; X_2^T, \ldots, \; X_{n-m}^T\right]^T$. The Lyapunov equation 29 is also written for entire system as follows:

$$A^T P + PA = -Q, \; PB = C^T \tag{34}$$

where

$$P = diag\left(P_1, P_2, \ldots, P_{n-m}\right),$$
$$Q = diag\left(Q_1, Q_2, \ldots, Q_{n-m}\right), \tag{35}$$

In order to design the robust control $v_R \in \Re^{n-m}$, it is assumed that $\left\| L_\xi L_f h(x) \right\| \leq \rho(q, v)$ where $\rho(q, v)$ is an upper bounding function. Considering Eqs. 10 and 13, $L_\xi L_f h(x)$ is calculated as follows:

$$L_\xi L_f h(x) = -J_h(q)\, S(q)\, \overline{M}^{-1} \times \left(\left(\overline{C}\left(q, \dot{q}\right) + k_2 \overline{B} X_T\right) v(t) + \overline{F}\left(\dot{q}\right) + \overline{\tau}_d\right) \tag{36}$$

where $J_h(q) = \left[J_{h1}^T(q), \; J_{h2}^T(q), \ldots, \; J_{h\,n-m}^T(q)\right]^T$ is the Jacobian matrix which is made up of Jacobians of all output equations with respect to q. By considering Eq. 36 and the structural properties of nonholonomic systems (see the property 2), one may conclude that

$$\left\| L_\xi L_f h(x) \right\| \leq \alpha_1 + \alpha_2 \|v\| + \alpha_3 \|v\|^2 \tag{37}$$

Therefore, the bounding function is obtained as $\rho(v) = \alpha_1 + \alpha_2 \|v\| + \alpha_3 \|v\|^2$ which can be defined in the parametric form, $\rho(v) = Y(v)\alpha$, where

$$Y(v) = \left[1 \;\; \|v\| \;\; \|v\|^2\right], \; \alpha = \left[\alpha_1 \; \alpha_2 \; \alpha_3\right]^T \tag{38}$$

and α is a vector of unknown constants of the bounding function.

3.2 Stability Analysis

The following theorem is presented to solve the integrated kinematic and dynamic trajectory tracking control problem of nonholonomic robotic systems in presence of both parametric and nonparametric uncertainties based on Assumptions 1 and 2.

Theorem 2 *Provided that the reference trajectory $y_r(t)$ is selected to be bounded for all times $t >$ 0, under Assumptions 1–3, the following adaptive-robust tracking controller guarantees that all signals in the closed-loop system are bounded and the position and velocity tracking errors, e_j and $\dot{e}_j$, $j = 1, 2, \ldots, n-m$ are uniformly ultimately bounded (UUB) and exponentially converge to a small ball containing the origin:*

$$u_a = \widehat{D}^{-1}(x)\left(\ddot{y}_r - K_p e - K_v \dot{e} - K_a \int_0^t e(\tau)\, d\tau - E_1 \widehat{\rho}^2 / \left(\widehat{\rho}\, \|E_1\| + \gamma(t)\right) - L_f^2 h\right),$$
$$\dot{\widehat{\theta}} = \Gamma_1 W^T E_1 - \Gamma_1 \sigma_1 \left(\widehat{\theta} - \theta_0\right),$$
$$\dot{\widehat{\alpha}} = \Gamma_2 Y^T \|E_1\| - \Gamma_2 \sigma_2 \left(\widehat{\alpha} - \alpha_0\right), \; \widehat{\rho}(v) = Y(v)\, \widehat{\alpha} \tag{39}$$

where $\widehat{D}(x)$ denotes the estimation of decoupling matrix which is defined by Eq. 20, $W \in \Re^{(n-m)\times p}$ is the regression matrix, $E_1 \in \Re^{n-m}$ is a vector of filtered error signals and $\Gamma_1 \in \Re^{p\times p}$ and $\Gamma_2 \in \Re^{3\times 3}$ are symmetric and positive definite matrices as the adaptive gains. $K_p \in \Re^{(n-m)\times(n-m)}$, $K_v \in \Re^{(n-m)\times(n-m)}$ and $K_a \in \Re^{(n-m)\times(n-m)}$ are diagonal matrices which denote proportional, derivative and *integral gains of the linear control law for the entire system, respectively. The parameters σ_1 and σ_2 are small positive constants and $\gamma(t)$ is a positive time function which is assumed to be constant here. The parameters θ_0 and α_0 are also the priori estimates of the parameters θ and α.*

Proof Consider the following Lyapunov function

$$V\left(X,\widetilde{\theta},\widetilde{\alpha}\right)=1/2\left(X^TPX+\widetilde{\theta}^T\Gamma_1^{-1}\widetilde{\theta}+\widetilde{\alpha}^T\Gamma_2^{-1}\widetilde{\alpha}\right) \tag{40}$$

where $\widetilde{\alpha}=\alpha-\widehat{\alpha}$ and $\widetilde{\theta}=\theta-\widehat{\theta}$. By differentiating Eq. 40 and applying Eqs. 32 and 34, one gets

$$\begin{aligned}\dot{V}\left(X,\widetilde{\theta},\widetilde{\alpha}\right)&=-1/2X^TQX\\&\quad+\widetilde{\theta}^T\left(W^TE_1+\Gamma_1^{-1}\dot{\widetilde{\theta}}\right)+v_R^TE_1\\&\quad+\left(L_\xi L_fh(x)\right)^TE_1+\widetilde{\alpha}^T\Gamma_2^{-1}\dot{\widetilde{\alpha}}\end{aligned} \tag{41}$$

Considering the adaptation laws in Eq. 39 and $\dot{\widetilde{\theta}}=-\dot{\widehat{\theta}}$ and $\dot{\widetilde{\alpha}}=-\dot{\widehat{\alpha}}$, Eq. 41 is written as

$$\begin{aligned}\dot{V}\left(X,\widetilde{\theta},\widetilde{\alpha}\right)&=-1/2X^TQX+\widetilde{\theta}^T\sigma_1\left(\widehat{\theta}-\theta_0\right)\\&\quad+v_R^TE_1+\left(L_\xi L_fh(x)\right)^TE_1\\&\quad-\widetilde{\alpha}^TY^T\|E_1\|+\widetilde{\alpha}^T\sigma_2\left(\widehat{\alpha}-\alpha_0\right)\end{aligned} \tag{42}$$

By using the parametric form of the upper bound of $L_\xi L_fh(x)$, i.e. $\rho=Y\alpha$, one obtains

$$\begin{aligned}\dot{V}\left(X,\widetilde{\theta},\widetilde{\alpha}\right)&\le-1/2X^TQX+v_R^TE_1\\&\quad+\alpha^TY^T\|E_1\|-\widetilde{\alpha}^TY^T\|E_1\|\\&\quad+\widetilde{\theta}^T\sigma_1\left(\widehat{\theta}-\theta_0\right)+\widetilde{\alpha}^T\sigma_2\left(\widehat{\alpha}-\alpha_0\right)\end{aligned} \tag{43}$$

Then, by choosing the robust control law as $v_R=-E_1\widehat{\rho}^2/(\widehat{\rho}\|E_1\|+\gamma)$ and substituting it in Eq. 43, the following inequality is achieved

$$\begin{aligned}\dot{V}\left(X,\widetilde{\theta},\widetilde{\alpha}\right)&\le-1/2X^TQX+\frac{Y\widehat{\alpha}\|E_1\|\gamma}{Y\widehat{\alpha}\|E_1\|+\gamma}\\&\quad+\widetilde{\theta}^T\sigma_1\left(\widehat{\theta}-\theta_0\right)+\widetilde{\alpha}^T\sigma_2\left(\widehat{\alpha}-\alpha_0\right).\end{aligned} \tag{44}$$

Since

$$0\le Y\widehat{\alpha}\|E_1\|\gamma/(Y\widehat{\alpha}\|E_1\|+\gamma)\le\gamma \tag{45}$$

and considering that $\widehat{\theta}=\theta-\widetilde{\theta}$ and $\widehat{\alpha}=\alpha-\widetilde{\alpha}$, one may write Eq. 44 as follows:

$$\begin{aligned}\dot{V}\left(X,\widetilde{\theta},\widetilde{\alpha}\right)&\le-1/2X^TQX+\gamma+\widetilde{\theta}^T\sigma_1\left(\theta-\theta_0\right)\\&\quad-\widetilde{\theta}^T\sigma_1\widetilde{\theta}+\widetilde{\alpha}^T\sigma_2\left(\alpha-\alpha_0\right)-\widetilde{\alpha}^T\sigma_2\widetilde{\alpha}\end{aligned} \tag{46}$$

Now, by completing the square terms in Eq. 46 and considering the minimum singular value of the matrix Q, i.e. $\mu_Q=\sqrt{\lambda_{\min}\left(Q^TQ\right)}$, one gets

$$\begin{aligned}\dot{V}\left(X,\widetilde{\theta},\widetilde{\alpha}\right)&\le-1/2\mu_Q\|X\|^2\\&\quad-\mu_1\left(1-0.5/\kappa^2\right)\left\|\widetilde{\theta}\right\|^2\\&\quad+1/2\mu_1\kappa^2\|\theta-\theta_0\|^2\\&\quad-\mu_2\left(1-0.5/\kappa^2\right)\|\widetilde{\alpha}\|^2\\&\quad+1/2\mu_2\kappa^2\|\alpha-\alpha_0\|^2+\gamma.\end{aligned} \tag{47}$$

where $\mu_j=\sqrt{\lambda_{\min}\left(\sigma_j^T\sigma_j\right)}$ shows the minimum singular value of the matrix σ_j. By defining the following parameters,

$$\begin{aligned}&\nu_1=1/2\mu_Q>0,\ \ \nu_2=\mu_1\left(1-0.5/\kappa^2\right)>0,\\&\nu_3=\mu_2\left(1-0.5/\kappa^2\right)>0,\\&\varepsilon=1/2\mu_1\kappa^2\|\theta-\theta_0\|^2+1/2\mu_2\kappa^2\|\alpha-\alpha_0\|^2+\gamma,\end{aligned} \tag{48}$$

where $\kappa>\sqrt{2}/2$, inequality 47 is re-written as follows:

$$\dot{V}\left(X,\widetilde{\theta},\widetilde{\alpha}\right)\le-\nu_1\|X\|^2-\nu_2\left\|\widetilde{\theta}\right\|^2-\nu_3\|\widetilde{\alpha}\|^2+\varepsilon \tag{49}$$

On the other hand, from Eq. 40 and the fact that

$$\lambda_{\min}(P)\|z\|^2\le z^TPz\le\lambda_{\max}(P)\|z\|^2 \tag{50}$$

for any $z(t) \in \Re^n$, inequality 49 becomes

$$\dot{V}\left(S(t), \widetilde{\theta}(t), \widetilde{\alpha}(t)\right) \leq -c_v V\left(S(t), \widetilde{\theta}(t), \widetilde{\alpha}(t)\right) + \varepsilon \tag{51}$$

where

$$c_v = \min\left\{2\nu_1/\lambda_{\max}(P),\ 2\nu_2/\lambda_{\max}\left(\Gamma_1^{-1}\right), 2\nu_3/\lambda_{\max}\left(\Gamma_2^{-1}\right)\right\}, \tag{52}$$

Solving the differential inequality 51 yields

$$0 \leq V(t) \leq V(t_0)\,e^{-c_v t} + \varepsilon/c_v\left(1 - e^{-c_v t}\right), \quad \forall t \in [0,\ \infty) \tag{53}$$

From Eq. 53, it is obvious that the Lyapunov function is upper bounded by

$$V(t) \leq \max\left\{V(t_0),\ \varepsilon/c_v\right\}, \quad \forall t \geq 0 \tag{54}$$

which together with the definition of $V(t)$ in Eq. 40 results in

$$\|X(t)\| \leq \sqrt{2\max\left\{V(t_0),\ \varepsilon/c_v\right\}/\lambda_{\min}(P)}, \tag{55}$$

Equation 53 means that $V(t)$ is eventually bounded by ε/c_v. Equation 49 implies that $\dot{V}(t)$ is strictly negative when $\varepsilon \leq \nu_1\|X\|^2$ which means that $\dot{V} < 0$ outside the compact set $\Omega_X = \left\{X(t)\middle|\,\|X(t)\| \leq \sqrt{\varepsilon/\nu_1}\right\}$. As a result, $\|X(t)\|$ decreases whenever $X(t)$ is outside the compact set Ω_X, and hence $\|X(t)\|$ is UUB. This discussion implies that tracking errors are UUB and exponentially converge to a small ball containing the origin. Considering Eqs. 12, 13 and Assumption 2, since $y_r(t),\ \dot{y}_r(t),\ e(t),\ \dot{e}(t) \in L_\infty$, one may conclude that $q(t),\ v(t) \in L_\infty$. The presented stability analysis demonstrates that a guaranteed transient performance and final tracking accuracy is obtained since the exponential decaying rate c_v and the radius of the ball of final tracking errors can be freely adjusted by the design parameters $\Gamma_1,\ \Gamma_2,\ K_p,\ K_v,\ K_a,\ \theta_0,\ \alpha_0$ and γ. □

Remark 1 The determinant of decoupling matrix, $\widehat{D}(x)$, in the control law in Eq. 39 may include some of estimated parameters $\widehat{\theta}$. Thus, prior bounds on these parameters are sufficient to guarantee non-singularity of the decoupling matrix. As implied in Sastry's work [2], several techniques such as projection operator exist in the literature for this purpose [12].

Remark 2 The leakage modification for adaptation law for the estimated parameter $\widehat{\alpha}$ in Eq. 39 is necessary for robustness enhancement. This modification guarantees boundedness of the estimated parameter vector $\widehat{\alpha}$ to provide an upper bound for the uncertainty $L_\xi L_f h(x)$ for applying in the robust control law v_R [11].

Remark 3 One may compromise between the final tracking accuracy and smoothness of the control signal by tuning of $\gamma(t)$ in Eq. 39. The robust control v_R can be made smoother by selecting a larger value for $\gamma(t)$. However, larger values of $\gamma(t)$ may result in a larger ultimate bound. One may choose an appropriate time function for $\gamma(t)$ to tune the smoothness of the control signal and the tracking accuracy. For example, since the uncertainty is large in the initial time of the tracking, it demands high control activity of the robotic system actuators due to the chattering. Thus, the choice of

$$\gamma(t) = \begin{cases} \gamma_1, & \text{if } 0 \leq t \leq T \\ \gamma_2 + \gamma_1 e^{-c(t-T)} & \text{if } t > T, \end{cases}$$

with $\gamma_1,\ \gamma_2,\ c > 0$ (where $\gamma_1 >> \gamma_2$) helps hold the boundary layer thickness $\gamma(t)$ at a large value at the start-up time in order to prevent the actuators chattering and saturation. Then, $\gamma(t)$ decreases with time which helps preserve the final tracking accuracy.

Remark 4 The proposed control scheme can be extended to other kinds of controllers in the outer loop by defining the auxiliary filtered tracking error $\varepsilon(t) \in \Re^{n-m}$ in Eq. 27 as $\varepsilon(s) = \Lambda^{-1}(s))\,e(s)$ where

$$\Lambda^{-1}(s) = \left[s\,I_{n-m} + \frac{1}{s}K(s)\right]$$

where s is the Laplace transform variable and the gain matrix $K(s)$ is chosen such that $\Lambda(s)$ is a strictly proper, stable transfer function matrix.

Note that $K(s)$ must be chosen such that $\varepsilon(t)$ does not depend on the measurement of $\ddot{y}$. For this purpose, $\Lambda(s)$ is selected such that it has a relative degree of one. Various controllers may be developed by different choices of the matrix $K(s)$.

Remark 5 Since most of commercially available WMRs are well equipped with navigational sensors, Assumption 1 is always satisfied. However, as frequently reported in the literature [31, 32], the use of a velocity observer is necessary from practical viewpoints such as a cost-effective implementation which is not the subject of this study. The boundedness of the reference trajectory and its derivatives up to the second order in Assumption 2 is restrictive to choose every desired trajectory in real world implementation scenarios. However, it is necessary for the presented theoretical developments.

4 Simulation Study on a Nonholonomic WMR

This section presents the application of the proposed control law in Section 3 on a nonholonomic differential drive wheeled mobile robot. The computer simulation results are also presented to evaluate the efficacy of the controller. The configuration of a differential drive WMR is shown in Fig. 1. The WMR has two conventional fixed wheels on a single common axle and a castor wheel to maintain the equilibrium of the robot. The centre of mass of the robot is located in $P_C = (x_C, y_C)$. The point $P_0 = (x_O, y_O)$ is the origin of the local coordinate frame that is attached to the WMR body and is located at a distance d from P_C. The point $P_L = (x_L, y_L)$ is a virtual reference point on $x$axis of the local frame at a distance L (look-ahead distance) of P_O [8]. The parameter $2b$ is the distance between two fixed wheels. The radius of each wheel is denoted by r. If the generalized coordinates vector is selected to be $q = [x_O, y_O, \phi]^T$, one velocity constraint is obtained as $\dot{y}_O \cos\phi - \dot{x}_O \sin\phi = 0$. Thus, pseudo-velocities of the nonholonomic WMR are defined as $v(t) = [v_1(t),\ v_2(t)]^T$ which v_1 and v_2

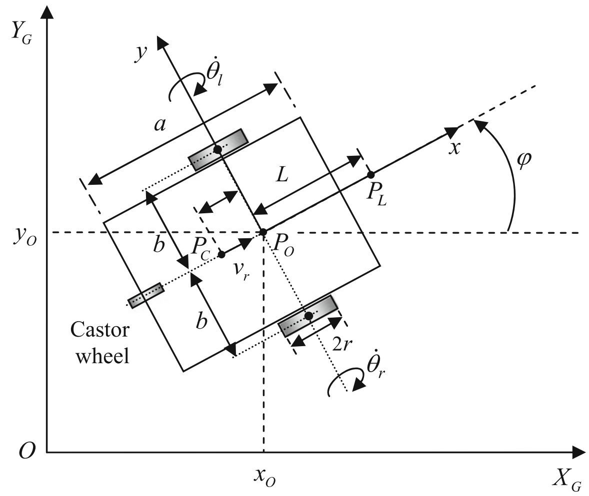

Fig. 1 Configuration of a differential drive wheeled mobile robot

denote the linear and angular velocities of the robot, respectively. According to the notation introduced before, the following kinematic and dynamic matrices are obtained:

$$S(q) = \begin{bmatrix} \cos\phi & 0 \\ \sin\phi & 0 \\ 0 & 1 \end{bmatrix},\ \overline{M} = \begin{bmatrix} m & 0 \\ 0 & I \end{bmatrix},$$

$$\overline{C} = \begin{bmatrix} 0 & m_C d \dot{\phi} \\ -m_C d \dot{\phi} & 0 \end{bmatrix},\ X_T = \begin{bmatrix} 1/r & b/r \\ 1/r & -b/r \end{bmatrix}, \tag{56}$$

where $m = m_C + 2m_w$, $I = I_C + 2I_m + m_C d^2 + 2m_w b^2$ and $\overline{B} = X_T^T$. The parameter m_c is the mass of the platform without the driving wheels and the rotors of the DC motors, m_w denotes the mass of each driving wheel plus the rotor of its motor, I_c denotes the moment of inertia of the platform without the driving wheels and the rotors of the motors about a vertical axis through P_C and I_m is the moment of inertia of each wheel and the motor rotor about a wheel diameter.

The voltage inputs of the right and left motors of the differential drive WMR is denoted by $u_a = [u_{a1},\ u_{a2}]^T$. Inertia parameters (mass and moment of inertia) and actuators parameters $(k_1,\ k_2)$ are supposed to be uncertain. Then, by substituting Eq. 56 in Eq. 10, and defining the new uncertain parameters as $\theta_1 = k_1/m$ and $\theta_2 = k_1/I$, one obtains

$$\begin{aligned} f(x) &= \left[v_1 \cos\phi \; v_1 \sin\phi \; v_2 \; 0 \; 0\right]^T, \\ g_1(x,\theta) &= \left[0\;0\;0\;\theta_1/r \;\; \theta_2 b/r\right]^T, \\ g_2(x,\theta) &= \left[0\;0\;0\;\theta_1/r \;\; -\theta_2 b/r\right]^T \end{aligned} \tag{57}$$

The following output variables are chosen to track a desired trajectory based on Look-ahead control method ($n - m = 2$):

$$\begin{aligned} y = h(x) &= \left[h_1(q),\; h_2(q)\right]^T \\ &= \left[x_O + L\cos\phi,\; y_O + L\sin\phi\right]^T \end{aligned} \tag{58}$$

After calculation of $L_f^2 h(x)$ and $\widetilde{D}(x)\,\widehat{D}^{-1}(x)$ in Eq. 22,

$$L_f^2 h(x) = \partial/\partial q\left(J_h(q)\,S(q)\,v\right) S(q)\,v, \tag{59}$$

$$\widetilde{D}(x)\,\widehat{D}^{-1}(x) = \begin{bmatrix} \widetilde{\theta}_1\widehat{\theta}_1^{-1}\cos^2\phi + \widetilde{\theta}_2\widehat{\theta}_2^{-1}\sin^2\phi & \left(\widetilde{\theta}_1\widehat{\theta}_1^{-1} - \widetilde{\theta}_2\widehat{\theta}_2^{-1}\right)\cos\phi\sin\phi \\ \left(\widetilde{\theta}_1\widehat{\theta}_1^{-1} - \widetilde{\theta}_2\widehat{\theta}_2^{-1}\right)\cos\phi\sin\phi & \widetilde{\theta}_1\widehat{\theta}_1^{-1}\sin^2\phi + \widetilde{\theta}_2\widehat{\theta}_2^{-1}\cos^2\phi \end{bmatrix} \tag{60}$$

the regression matrix in Eq. 24 is obtained as follows:

$$W = \begin{bmatrix} \widehat{\theta}_1^{-1}\left(\Phi_1\cos^2\phi + \Phi_2\sin\phi\cos\phi\right) & \widehat{\theta}_2^{-1}\left(\Phi_1\sin^2\phi - \Phi_2\sin\phi\cos\phi\right) \\ \widehat{\theta}_1^{-1}\left(\Phi_1\sin\phi\cos\phi + \Phi_2\sin^2\phi\right) & \widehat{\theta}_2^{-1}\left(-\Phi_1\sin\phi\cos\phi + \Phi_2\cos^2\phi\right) \end{bmatrix} \tag{61}$$

where

$$\begin{aligned} \Phi_1 &= \eta_1 - \partial/\partial q\left(J_{h1}\,Sv\right) Sv, \\ \Phi_2 &= \eta_2 - \partial/\partial q\left(J_{h2}\,Sv\right) Sv. \end{aligned} \tag{62}$$

The block diagram of the inverse dynamics controller is shown in Fig. 2. Some computer simulations were performed in order to show the tracking performance and robustness of the proposed controller under parametric and nonparametric uncertainties. The WMR parameters are chosen to match with a real world mobile robot, and Gaussian white noise is also added to the states to simulate a localization system. All simulations are carried out based on Euler approximation with a time step of 20 ms. Real physical parameters of the WMR and control parameters are listed as follows: $r = 0.1m$, $b = 0.3m$, $d = 0.05m$, $L = 0.1m$, $m_C = 10Kg$, $m_w = 0.2Kg$, $I_m = 0.006Kg.m^2$, $I_C = 3Kg.m^2$, $k_1 = k_2 = 0.20$. Based on the SPR conditions of the system 28 which are presented in the Section 3 in order to guarantee SPR-Lyapunov stability of the closed-loop system, the controller parameters are set to $k_p = 1$, $k_v = 2$, $k_a = 0.2$ and $\beta_1 = 0.5$, $\beta_1 = 0.1$. Adaptation gains in Eq. 39 are chosen as $\Gamma_1 = diag\left([1, 1]\right)$, $\Gamma_2 = diag\left([1,\ 1,\ 1]\right)$. Other remaining control parameters are selected as $\sigma_1 = 0.005$, $\sigma_2 = 0.005$, $\gamma = 10$, $\alpha_0 = 0$, $\theta_0 = 0$. An eight-shape trajectory is considered as the reference input which is specified by $y_{1r}(t) = x_g + R\sin(2\omega_r t)$ and $y_{2r}(t) = y_g + R\sin(\omega_r t)$ where $\left(x_g,\ y_g\right) = (2.5m,\ 5.5m)$, $R = 2m$ and $\omega_r = 0.05$. The initial conditions are assumed to be $x(0) = 3m$; $y(0) = 6.5m$; $\phi(0) = -30^0$; $v_1(0) = 0$; $v_2(0) = 0$. To evaluate the effectiveness of the proposed control law, it is assumed that inertia parameters have 15–20% uncertainty, the coulomb and viscose frictions are considered such that $\left\|\overline{F}\left(\dot{q}\right)\right\| \le 0.5 + 0.8\left\|v\right\|$, a sinusoidal dynamic disturbance is considered as $\overline{\tau}_d = \left[3\sin\left(t/20\right),\ 3\sin\left(t/20\right)\right]^T$.

The actuator control signal is saturated to lie within $|u_a| \le 24V$. Computer simulations were successfully carried out over and over for different set of WMR paremeters, control parameters and reference trajectories. Some results are arbitrarily selected based on aforementioned parameters and

Fig. 2 Block diagram of the proposed controller

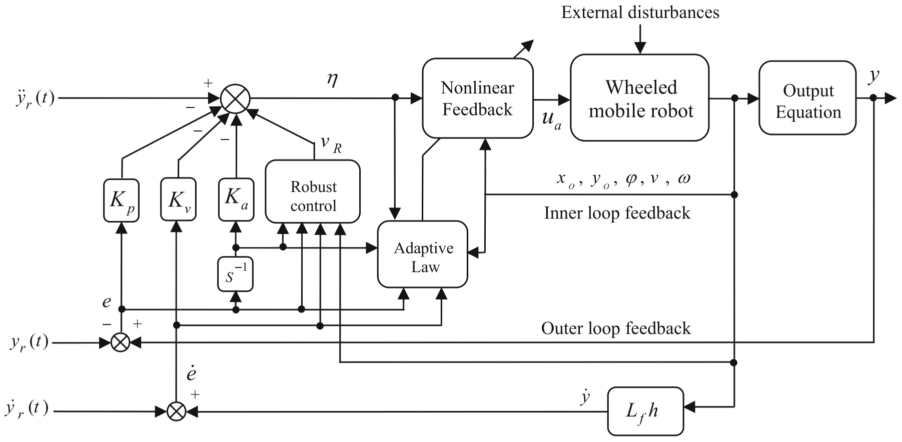

reported by Figs. 3 and 4. As shown by these figures, the proposed adaptive-robust feedback linearizing (ARFL) controller shows better tracking performance and robustness than the proposed adaptive feedback linearizing (AFL) controller in [27]. However, the adaptive controller generates smoother control signal as shown by the Fig. 5. Figure 6 shows that the chattering phenomenon is inevitable in the control signal of the proposed adaptive-robust controller. The saturation-type control in Eq. 39 can be made smoother by selecting a larger value for the parameter γ. However, larger value of γ increases the value of ε in Eq. 55 which may result in a larger ultimate bound. One may choose an appropriate function for the parameter γ to have a trade-off between smoothness of the control and the tracking accuracy.

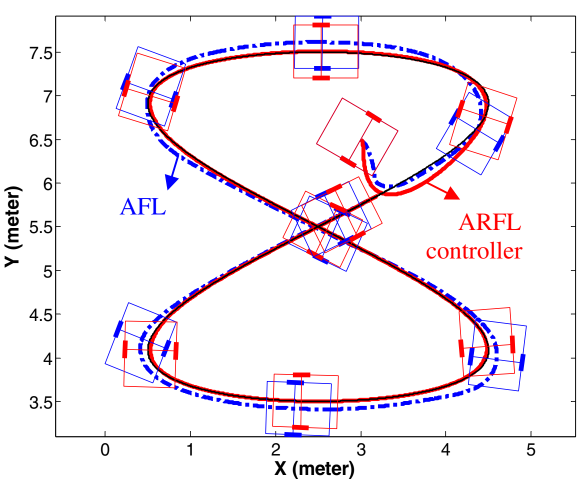

Fig. 3 Generated trajectories by adaptive feedback linearizing controller (*dashed line*) and adaptive-robust feedback linearizing controller (*bold solid line*)

5 Experimental Studies on a Commercial WMR

The robuLAB 10 wheeled mobile robot is employed to experimentally evaluate the proposed controller (Eq. 39). The robuLAB is a differential drive WMR which is manufactured by Robosoft Inc. Figure 7 shows the feature of the WMR whose size is 450 mm × 400 mm × 243 mm. The planar configuration of the robuLAB 10 is exactly illustrated by Fig. 1. The WMR is equipped with two rings of ultrasonic sensors, a URG-04LX laser range finder, a wireless LAN for the communication, 12V batteries, and two DC motors which are connected to the wheels through a 5.5:1 reduction gear box. Each wheel is equipped with an incremental encoder for the localization system which updates the relative pose of the WMR every 200 ms. Thus, the sampling time of the controller is limited by this value in real experiments. The measured distance between each driving wheel and the axis of the symmetry is 187.5 mm. The radius of each wheel is also measured as 72.5 mm. Two passive castor wheels are placed in the rear and front of the WMR to preserve its equilibrium. The WMR payload is reported to be 30 kg. The open-loop experiments show that the maximum linear and angular velocities of the WMR are 4 m/s and 0.5 rad/s, respectively. This WMR does not accept the motors voltage as the input. It is only

Fig. 4 Tracking errors for adaptive feedback linearizing controller (*dashed line*) and adaptive-robust feedback linearizing controller (*solid line*)

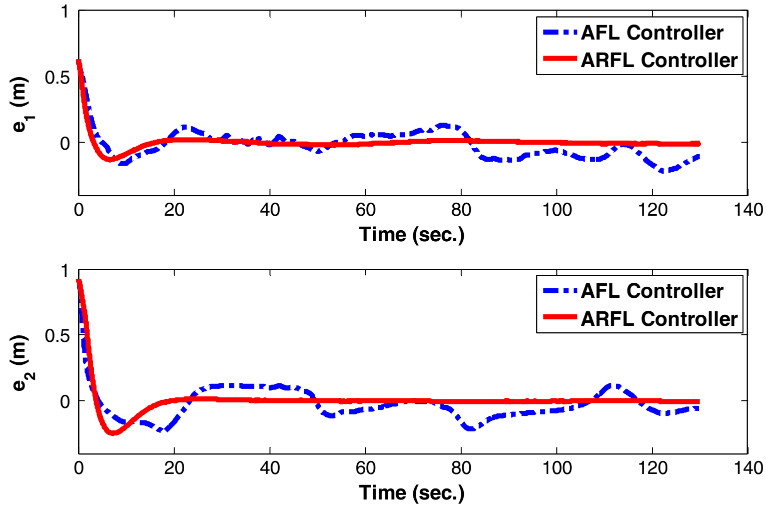

Fig. 5 Control signals for the adaptive controller

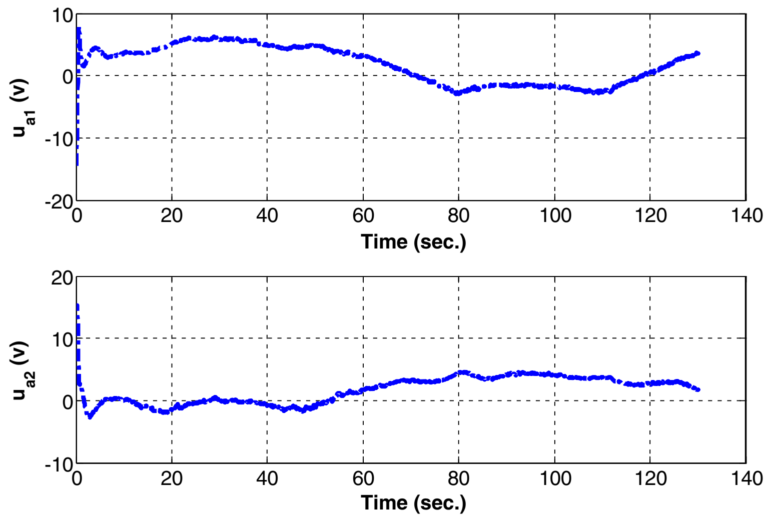

Fig. 6 Control signals for the adaptive-robust controller

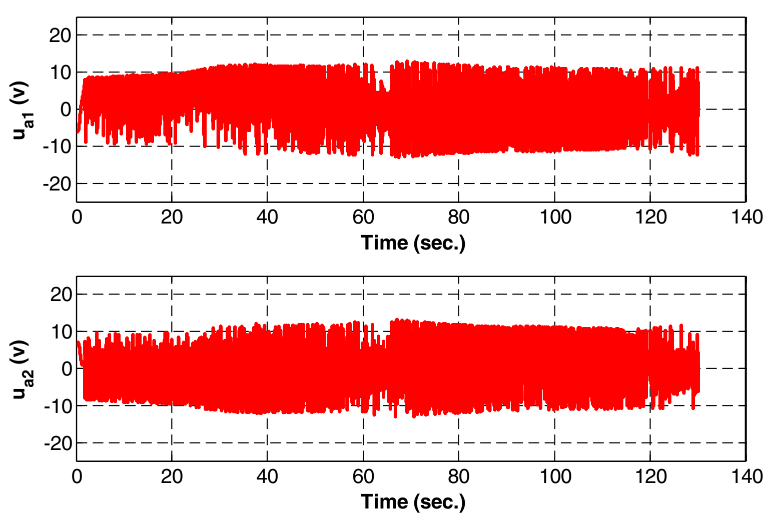

Fig. 7 RobuLAB 10 wheeled mobile platform

commanded by linear and angular velocities which are denoted by $v_{ref,1}(t)$ and $v_{ref,2}(t)$, respectively. Therefore, in order to test the proposed control law 39 experimentally, the following model is used which is presented by De La Cruz et al. [23]:

$$\dot{x} = f(x) + g_1(x,\theta)\, v_{ref,1} + g_2(x,\theta)\, v_{ref,2} + \xi(x), \tag{63}$$

where $f(x)$ is the same as Eq. 57, the output equations is selected as Eq. 58 and

$$g_1(x,\theta) = \left[0\ 0\ 0\ \theta_1\ 0\right]^T, g_2(x,\theta) = \left[0\ 0\ 0\ 0\ \theta_2\right]^T,$$
$$\xi(x) = \begin{bmatrix} 0\ 0\ 0 & p_1 v_2^2 - p_2 v_1 + \delta_{v_1} \\ & -p_3 v_1 v_2 - p_4 v_2 + \delta_{v_2} \end{bmatrix}^T, \tag{64}$$

and $x = \left[x,\ y,\ \phi,\ v_1,\ v_2\right]^T$ denotes the state vector, p_i, $i = 1, \ldots, 4$ are unknown constant parameters, the terms δ_{v_1} and δ_{v_2} denote norm-bounded unstructured uncertainties due to frictions and unmodeled dynamics. The interested reader is referred to [23, 24] for more details about the above presented model. In this experiment, Microsoft Robotics Developer Studio (MRDS) is used to implement the proposed controller. The MRDS executes the controller program code on a host computer and generates the reference linear and angular velocities of the WMR. The host computer is a Pentium 4 processor which commands to RobuLAB 10 through a wireless LAN. The commanded velocities are fed to low-level controllers which are implemented on the robuLAB 10 robot. The pose (i.e. the position and orientation) measurements of the incremental encoders are fed back to the host computer via the WLAN. In order to estimate the WMR velocities from the pose measurements, a filtered derivative is used as follows

$$v_k = \alpha_d v_{k-1} + (q_k - q_{k-1})/T_s \tag{65}$$

where α_d is a design parameter, q_k is the WMR pose at k-th step and T_s denotes the sampling time. Different sources of uncertainties can be observed in this practical experience which some of them are listed as follows:

1) There is no knowledge about the inertia and actuators parameters of the WMR. This clearly shows parametric uncertainties in the WMR system. Moreover, in order to test the robustness of the controller, the robot is

Fig. 8 The desired trajectory (*dashed line*) and trajectory of the proposed controller (*bold solid line*) in $x - y$ plane

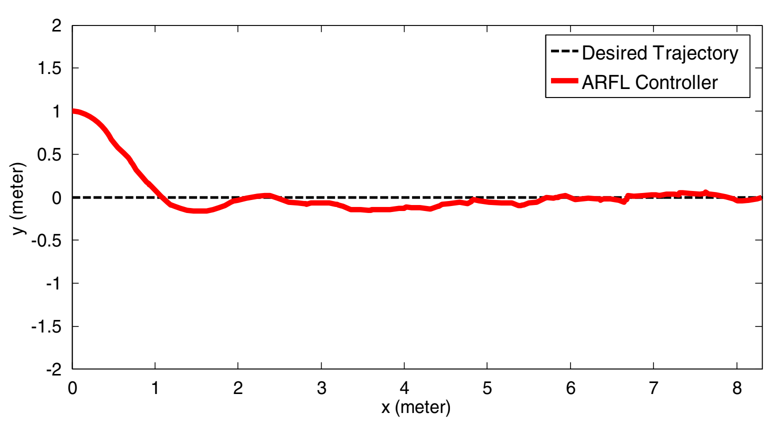

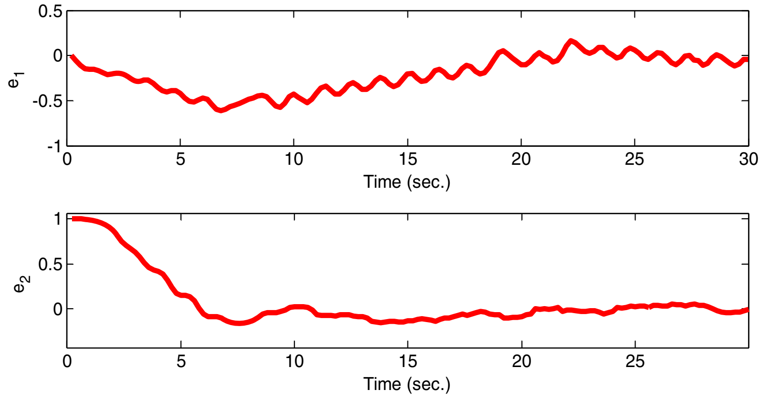

Fig. 9 The tracking errors for the proposed controller

loaded and unloaded by some objects during the motion.

2) The unmodeled castor wheels of the robuLAB 10 show undesirable effects on the motion of the WMR in the open-loop experiments. Their unmodeled dynamics are considered as a nonparametric uncertainty.
3) The wheels slippage and the friction of the rough ground surface also impose some nonparametric uncertainties to the WMR control system in these experiments.

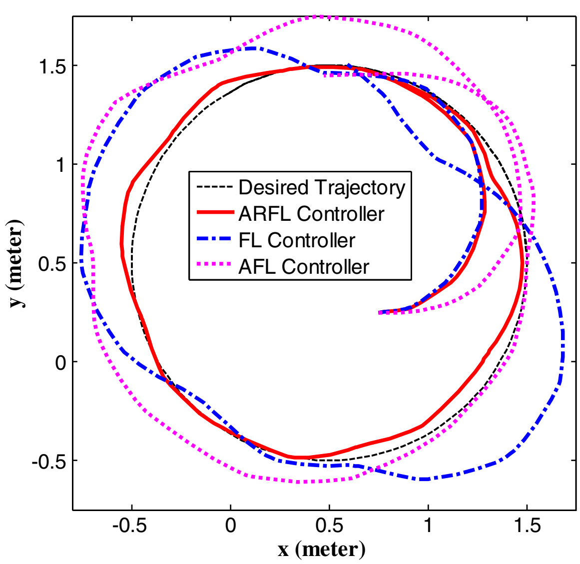

Fig. 10 The desired trajectory (*dashed line*), trajectories of non-adaptive controller (*dashed-dotted line*), the adaptive controller (*dotted line*) and the proposed controller (*bold solid line*) in $x - y$ plane

4) The control commands, which are sent to the WMR system via a wireless LAN, are inevitably contaminated with the additive noise in the environment.
5) The measurement error of the localization system is accumulated over the time which induces some source of uncertainty.
6) PD approximation errors in the model 62 impose an uncertainty to the WMR control system (see [23, 24] for more details).

According to the presented design procedure, an adaptive robust inverse dynamics controller is designed based on the model 63, 64 and 58. Then, the controller program code was written in C# programming language in the MRDS environment. The controller parameters for the experiment are chosen similar to simulation parameters.

In the first experiment, a line trajectory is considered as the reference input which is specified by $y_{1r}(t) = x_g + 0.275\,t\,[H(t) - H(t-30)]$ and $y_{2r}(t) = y_g$ where $(x_g,\ y_g) = (0,\ 0)$ and $H(\bullet)$ denotes the standard Heaviside step function. The initial values of WMR motion are set to $x(0) = 0$; $y(0) = 1m$; $\phi(0) = 0^0$; $v_1(0) = 0$; $v_2(0) = 0$. Figures 8 and 9 illustrate the line trajectory tracking results. As shown by the figures, the proposed controller shows a satisfactory tracking performance.

As a comparative study, another experiment has been performed. This time, a circle-shaped trajectory is considered as the reference input which is specified by $y_{1r}(t) = x_g + R\cos(\omega_r t)$, $y_{2r}(t) = y_g + R\sin(\omega_r t)$ where

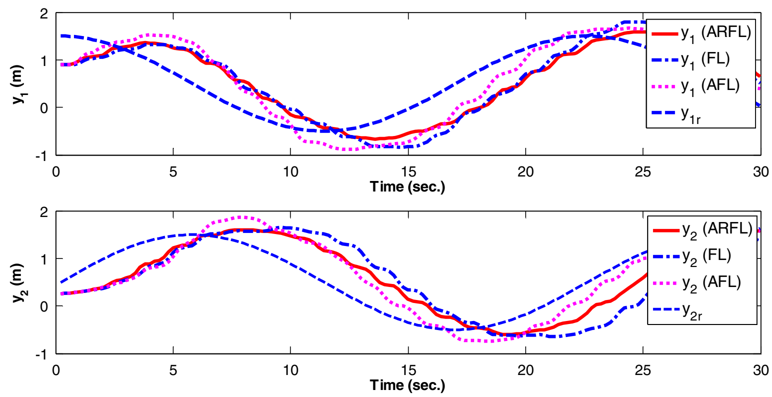

Fig. 11 The desired trajectory (*dashed line*), trajectories of non-adaptive controller (dashed-dotted line), the adaptive controller (*dotted line*) and the proposed controller (*bold solid line*)

$(x_g, y_g) = (0.5m, 0.5m)$ and $R = 1m$ represent the centre and radius of the circle, respectively. Note that ω_r must be chosen small because the controller performance degrades when ω_r is far from zero. The initial values of WMR motion are set to $x(0) = 0.75m$; $y(0) = 0.25m$; $\phi(0) = 0^0$; $v_1(0) = 0$; $v_2(0) = 0$. In order to evaluate the tracking performance and robustness of the proposed controller, a feedback linearizing control law without adaptation [8] and an adaptive feedback linearizing controller [27] are also tested on the WMR. Figure 10 illustrates one of experimental results which shows the desired trajectory (dashed line) and the trajectories of robuLAB 10 which are generated by all controllers. As shown in Figs. 10 and 11, experimental results also verify that the proposed controller in this paper is more effective than feedback linearizing controller and its adaptive version in the presence of parametric and nonparametric uncertainties. This shows that the feedback linearizing controller could not perfectly cancel the nonlinearities due to uncertainties. The adaptive controller could not also cope with the nonparametric uncertainties. However, in spite of the superiority of the proposed adaptive-robust controller in the experiments, the authors believe that the low bandwidth of the WMR actuators prevents the saturation-type adaptive robust part of the proposed controller (Eq. 39) to effectively perform regardless of the chattering in the control signal. Thus, this problem may restrict the proposed controller in a real experiment. As expressed before, the control signal can be made smoother by choosing a larger value for the parameter γ in Eq. 39 in expense of less tracking accuracy.

Figure 12 shows the control signals which are generated by the controllers. As shown by the figures, the saturation of the angular velocity at ±0.5rad/s prevents the proposed controller to obtain more satisfactory tracking results in comparison with simulations. Therefore, the actuators saturation and velocity constraints problem imposes some negative effects on the presented experimental results which must be treated by some existing solutions including anti-windup compensation, and the curvature constraints techniques [33]. Moreover, it should be noted that the castor wheels of robuLAB 10 with a notable suspension system intensely influence the presented experiments. Another problem with regard to the experimental results emerges from low-resolution encoder signals of robuLAB 10 whose numerical differentiation by the filtered derivative (Eq. 65) provides poor velocity approximations. The use of a velocity observer may solve this problem. However, one may achieve better results by well tuning of the controller parameters. In spite of the robustness of the proposed controller to parametric and nonparametric uncertainties, following problems also have undesirable effects in real experiments: non-idealities of the mechanical system such as backlash, wheel slippage, quantization errors, communication delays, PD approximation error of the WMR model in Eq. 63 (see [23] for more details) and especially low frequency of the odometry system which may induce some nonlinear effects in the closed-loop system.

Fig. 12 The generated control signals for the non-adaptive controller **a**, adaptive controller **b** and the proposed adaptive robust controller **c**

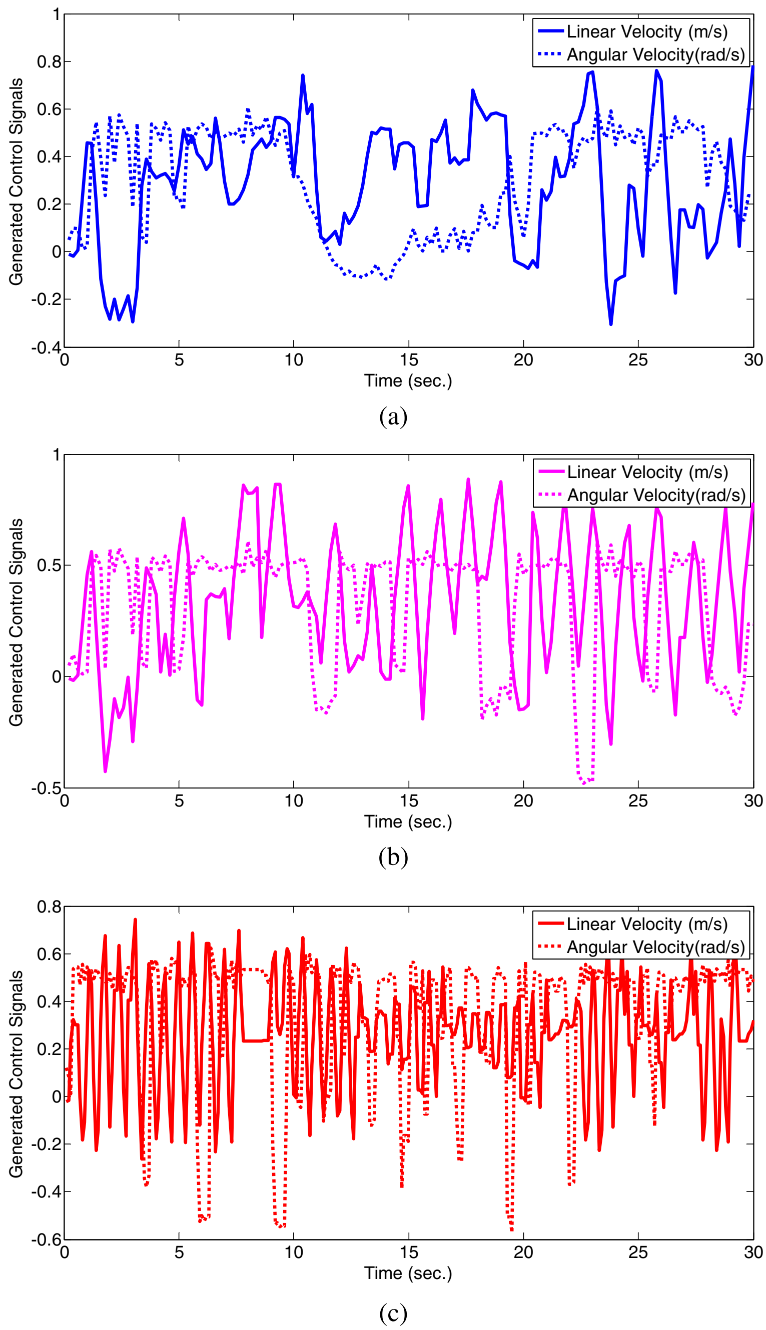

Improvement of the presented results demands more investigations which determine the direction of the future works in the next section.

6 Conclusions, Discussions and Future Works

In this note, the trajectory tracking problem of the nonholonomic robotic systems has been addressed. An adaptive-robust tracking control law has been proposed based on the inverse dynamics technique and the PID controller. Uniform ultimate boundedness stability of the position and velocity tracking errors was proved by SPR-Lyapunov stability analysis. Simulation results have been carried out to verify the effectiveness of the proposed controller. In order to confirm simulation results, some experiments were performed on robuLAB 10 mobile robot. Experimental results showed that the tracking performance and robustness of the proposed controller are better than those of the controllers in [8, 27]. Based on the presented experiments in the previous section, the following problems are emphasized to be addressed in the future works:

1. Unfortunately, incremental encoders of the WMR wheels are unreliable in the presence of sudden slippage of robot wheels. Furthermore, the sampling time of the experiment is restricted by the odometry sensors resolution which naturally prevents the user to achieve smaller tracking error bounds. In order to improve the experimental results, the application of extroceptive sensors, such as a fixed camera, is recommended for the future work.
2. Further researches will be focused on the actuators saturation problem to improve the tracking performance in real experiments. This problem is critical when the initial pose of the WMR is chosen far from the desired trajectory. Some solutions are the integrator anti-windup compensation in the outer loop of the controller and the curvature constraints techniques [33].
3. The performance of the proposed controller is reduced due to the chattering effects of the saturation-type controller and localization noise. As a result, future researches also devoted to these problems to improve the tracking performance of the proposed controller.
4. As mentioned before, since the boundedness of the reference trajectory and its derivatives up to the second order may not be really practical, the Assumption 2 make the proposed control approach to be restricted in real life applications. Therefore, removing of the Assumption 2 is the subject of next researches.
5. As depicted in the previous section, the WMR velocities are estimated from the pose measurements by a filtered derivative. In the case of a WMR with low frequency localization system (such as robuLAB 10), poor velocity approximations are provided in this way. Furthermore, there is no theoretical support to quantify the effects of such approximation in the stability of the closed-loop system. Thus, design of a velocity observer is highly recommended for the future work. As one may delve into the literature, there are little works [31, 32] to address an observer-based tracking controller for uncertain dynamic nonholonomic robotic systems.

Acknowledgements The authors would like to thank the Editor and the anonymous reviewers for their valuable comments for improving the original manuscript.

References

1. Brockett, R.W.: Asymptotic stability and fedback stabilization. In: Brockett, R.W., Milman, R.S., Sussman H.J. (eds.) Differential Geometric Control Theory, pp. 181–191. Boston (1983)
2. Sastry, S.S., Bodson, M.: Adaptive Control: Stability, Convergence and Robustness. Prentice-Hall, Englewood Cliffs, NJ (1989)
3. Campion, G., d'Andrea-Novel, B., Bastin, G.: Modeling and State Feedback Control of Nonholonomic Mechanical Systems. In: Proceedings of the 30th Conference on Decision and Control, IEEE, pp. 1184–1189. England (1991)
4. Campion, G., d'Andrea-Novel, B., Bastin, G.: Controllability and state feedback stabilization of nonholonomic mechanical systems. In: de Wit, C.C. et al. (eds.) Lecture Notes in Control and Information Science, vol. 162, pp. 106–124. Springer, New York (1991)
5. Bloch, A.M., Reyhanoglu, M., McClamroch, N.H.: Control and stabiliztion of nonholonomic dynamic systems. IEEE Trans. Automat. Contr. **37**(11), 1746–1757 (1992)
6. Yun, X., Kumar, V., Sarkar, N., Paljug, E.: Control of multiple arms with rolling constraints. In: Proceedings of the International Conference on Robotics and Automation, pp. 2193–2198 (1992)
7. Lewis, F.L., Abdallah, C.T., Dawson, D.M.: Contol of Robot Manipulators. MacMillan, New York (1993)
8. Sarkar, N., Yun, X., Kumar, V.: Control of mechanical systems with rolling constraint: application to dynamic control of mobile robots. Int. J. Rob. Res. **13**(1), 55–69 (1994)
9. Kolmanovsky, I., McClamroch, N.H.: Developments in nonholonomic control problems. IEEE Control Syst. Mag. **15**(6), 20–36 (1995)
10. Walsh, G., Bushnell, L.G.: Stabilization of multiple input chanied form control systems. Syst. Control Lett. **25**, 227–234 (1995)
11. Qu, Z., Dawson, D.M.: Robust Tracking Control of Robot Manipulators. IEEE Press, Piscataway, NJ (1996)

12. Ioannou, P.A., Sun, J.: Robust Adaptive Control. Prentice-Hall, Englewood Cliffs, NJ (1996)
13. Yun, X., Yamamoto, Y.: Stability analysis of the internal dynamics of a wheeled mobile robot. J. Robot. Syst. **14**, 697–709 (1997)
14. Yun, X., Sarkar, N.: Unified formulation of robotic systems with holonomic and nonholonomic constraints. IEEE Trans. Robot. Autom. **14**(4), 640–650 (1998)
15. Kim, D.-H., Oh, J.-H.: Tracking Control of a two-wheeled mobile robot using input-output linearization. J. Control Eng. Pract. **7**, 369–373 (1999)
16. Dong, W., Xu, W.L., Huo, W.: Trajectory tracking control of dynamic non-holonomic systems with unknown dynamics. Int. J. Robust Nonlinear Control **9**, 905–922 (1999)
17. Jiang, Z.-P., Nijmeijer, H.: A recursive technique for tracking control of dynamic nonholonomic systems in chained form. IEEE Trans. Automat. Contr. **34**(32), 265–279 (1999)
18. Dixon, W.E., Dawson, D.M.: Tracking and regulation control of a mobile robot system with kinematic disturbances: a variable structure-like approach. Trans. ASME J. Dyn. Syst. Measure. Control **122**, 616–623 (2000)
19. Dong, W., Xu, W.L.: Adaptive tracking control of uncertain nonholonomic dynamic system. IEEE Trans. Automat. Contr. **46**(3), 450–454 (2001)
20. Oriolo, G., De Luca, A., Vendittelli, M.: WMR control via dynamic feedback linearization: design, implementation, and experimental validation. IEEE Trans. Control Syst. Technol. **10**(6), 835–852 (2002)
21. Oya, M., Su, C.-Y., Katoh, R.: Robust adaptive motion/force tracking control of uncertain nonholonomic mechanical systems. IEEE Trans. Robot. Autom. **19**(1), 175–181 (2003)
22. Coelho, P., Nunes, U.: Lie algebra application to mobile robot control: a tutorial. Robotica **21**(5), 483–493 (2003)
23. De La Cruz, C., Carelli, R.: Dynamic modeling and centralized formation control of mobile robots. In: Proceedings of thirty-second annual conference of the IEEE industrial electronics society, pp. 3880–3885. IECON, Paris (2006)
24. Martins, F.N., Celeste, W.C., Carelli, R., Filho, M.S., Filho, T.F.B.: An adaptive dynamic controller for autonomous mobile robot trajectory tracking. J. Control Eng. Pract. **16**, 1354–1363 (2008)
25. Shojaei, K., Tarakameh, A., Mohammad Shahri, A.: Adaptive trajectory tracking of WMRs based on feedback linearization technique. In: Proceedings of the International Conference on Mechatronics and Automation, IEEE, pp. 729–734. Changchun, China (2009)
26. Shojaei, K., Mohammad Shahri, A., Tarakameh, A.: Adaptive feedback linearizing control of nonholonomic wheeled mobile robots in presence of parametric and nonparametric uncertainties. Robot. Comput.-Integr. Manuf. **27**, 194–204 (2011)
27. Shojaei, K., Mohammad Shahri, A., Tarakameh, A., Tabibian, B.: Adaptive trajectory tracking control of a differential drive wheeled mobile robot. Robotica **29**, 391–402 (2010)
28. Park, B.S., Yoo, S.J., Park, J.B., Choi, Y.H.: A simple adaptive control approach for trajectory tracking of electricaslly driven nonholonomic mobile robots. IEEE Trans. Control Syst. Technol. **18**(5), 1199–1206 (2010)
29. Chwa, D.: Tracking control of differential-drive wheeled mobile robots using a backstepping-like feedback linearization. IEEE Trans. Syst. Man Cybern. **40**(6), 1285–1295 (2010)
30. Das, T., Kar, I.N., Chaudhury, S.: Simple neuron-based adaptive controller for a nonholonomic mobile robot including actuator dynamics. J. Neurocomput. **69**, 2140–2151 (2006)
31. Park, B.S., Yoo, S.J., Park, J.B., Coi, Y.H.: Adaptive ouput-feedback control for trajectory tracking of eletcrically driven non-holonomic mobile robots. J. IET Control Theor. Appl. **5**(6), 830–838 (2010)
32. Shojaei, K., Shahri, A.M.: Output feedback tracking control of uncertain non-holonomic wheeled mobile robots: a dynamic surface control approach. J. IET Control Theor. Appl. **6**(2), 216–228 (2012)
33. Moustris, G.P., Tzafestas, S.G.: Switching fuzzy tracking control for mobile robots under curvature constraints. J. Control Eng. Pract. **19**(1), 45–53 (2011)